Japanese Journal of Applied Physics

The Japan Society of Applied Physics

BRIEF NOTES • OPEN ACCESS

Analytical formula for temperature dependence of resistivity in p-type 4H-SiC with wide-range doping concentrations

OPEN ACCESS

Japanese Journal of Applied Physics **57**, 088002 (2018)

https://doi.org/10.7567/JJAP.57.088002

BRIEF NOTE

Analytical formula for temperature dependence of resistivity in p-type 4H-SiC with wide-range doping concentrations

Satoshi Asada*, Jun Suda, and Tsunenobu Kimoto

Department of Electronic Science and Engineering, Kyoto University, Kyoto 615-8510, Japan

*E-mail: asada@semicon.kuee.kyoto-u.ac.jp

Received May 23, 2018; accepted May 30, 2018; published online June 29, 2018

Temperature dependence of resistivity from 250 to 900 K in p-type 4H-SiC with various doping concentrations (5.8×10^{14}–7.1×10^{18} cm^{-3}) was presented. The resistivity was obtained by the van der Pauw method in samples, whose doping concentrations were precisely determined in our previous work. From the experimental results, coefficients for a fitting formula with polynomial approximation were derived. We confirmed that the fitting formula can accurately estimate the resistivity of p-type SiC with wide-range doping concentrations.

4H-SiC is a promising semiconductor material for power devices because of its wide bandgap, high critical electric field, and high thermal conductivity.[1–4] Many studies have been performed to develop SiC power devices and their performance was significantly improved.[5–10] Aside from power-device applications, SiC devices are being recognized as attractive candidates for integrated circuits that can operate under harsh environmental conditions aiming at exploring Venus, underground drilling, controlling engine combustion, and so forth.[11–14]

For designing high-performance SiC devices or integrated circuits, the temperature dependence of electrical properties in SiC, such as mobility, carrier concentration, and resistivity, is of importance. The physical properties of n-type SiC have extensively been investigated so far,[15–19] and those of p-type SiC have also been obtained recently.[20–26] In our studies, the temperature dependences of hole mobility, hole concentration, and Hall scattering factor were shown by performing Hall-effect measurement on thick p-type SiC epilayers with various doping concentrations.[24,26] Although the resistivity of p-type SiC can be estimated from these data,[24,26] it is much more useful to give an analytical expression that describes the temperature dependence of resistivity. In this work, the temperature dependence of resistivity in p-type SiC with various doping concentrations is presented and analytical formulas describing resistivity are given.

Figure 1 shows the temperature dependence of resistivity in p-type SiC obtained by the van der Pauw method from 250 to 900 K. The aluminum (Al) doping concentration ranges from 5.8×10^{14} to 7.1×10^{18} cm^{-3} and the compensation ratio of all the samples is below 1% except for the sample with the lowest doping concentration ([Al] = 5.8×10^{14} cm^{-3}), the ratio of which is about 7%. Experimental details were described in our previous paper.[24] It becomes convenient when an analytical equation is derived for the precise estimation of resistivity in p-type SiC at arbitrary temperatures and doping concentrations. In the case of Si, the temperature and doping dependences of resistivity above 300 K are dominated by the temperature- and doping-dependent mobility because all the dopants in Si are almost completely ionized over 300 K. Thus, using empirical formulas for the temperature- and doping-dependent mobility, the resistivity of Si can be estimated.[27–30] However, as demonstrated in Fig. 1, the resistivity of p-type SiC strongly depends on the temperature and doping concentration, which is attributed to the large ionization energy of Al acceptors (~200 meV) and complicated carrier scattering mechanisms in SiC.[20,21,26] Thus, it is difficult to creat a simple equation or an empirical formula for the fitting. In order to acquire the fitting equation, the dependences of resistivity on the temperature and doping concentration should be considered separately.

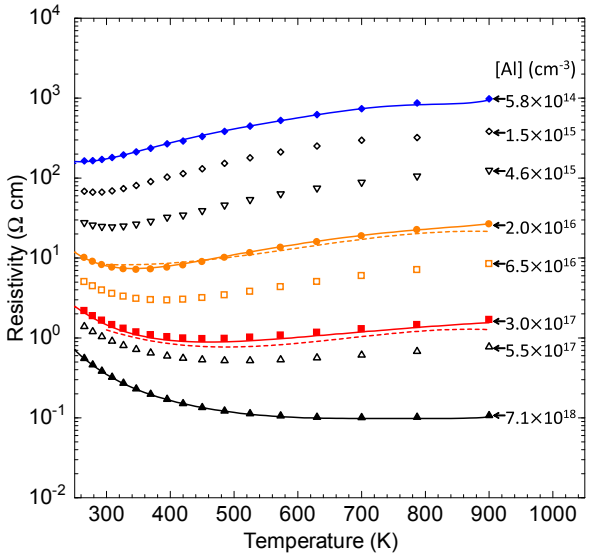

Fig. 1. (Color online) Temperature dependence of resistivity in p-type SiC with different Al-doping concentrations, as denoted for each Al density. The orange and red dotted lines are analytical curves calculated from Eqs. (1) and (2), and Table I for resistivity with doping concentrations of 2.0×10^{16} and 3.0×10^{17} cm^{-3}, respectively. The blue, orange, red, and black solid lines are fitting curves obtained from Eqs. (1) and (2), and Table II for resistivity with doping concentrations of 5.8×10^{14}, 2.0×10^{16}, 3.0×10^{17}, and 7.1×10^{18} cm^{-3}, respectively.

Figure 2(a) shows the dependence of resistivity on Al doping concentration at 293, 485, and 900 K. The resistivity of the samples with low doping concentrations (<2.0×10^{16} cm^{-3}) increased at high temperatures because almost all acceptors are ionized, while the mobility decreases due to enhanced phonon scattering.[20,21,26] On the other hand, the resistivity of the samples with high doping concentrations

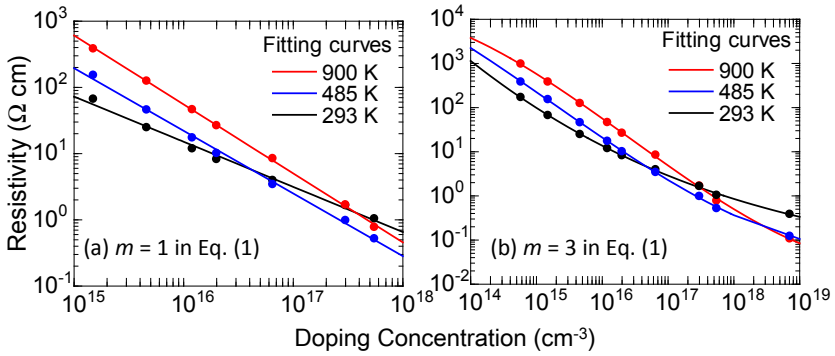

Fig. 2. (Color online) Dependence of resistivity on doping concentration. The black, blue, and red circles denote the experimental values at 293, 485, and 900 K, respectively. The black, blue, and red solid lines are fitting curves obtained by the (a) first- and (b) third-order polynomial approximations of Eq. (1).

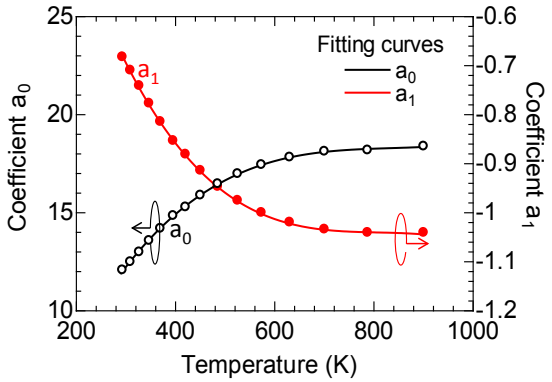

Fig. 3. (Color online) Temperature dependence of the coefficients a_0 and a_1 in Eq. (1), which are determined by the least-squares method applied to Fig. 2(a). The solid lines indicate the fitting curves obtained from the third-order polynomial approximation of Eq. (2).

($>2.0 \times 10^{16}\,\mathrm{cm}^{-3}$) did not monotonically increase with elevating the temperature because the increase in hole concentration compensates the decrease in mobility. A fitting formula for the doping concentration dependence of resistivity at every measurement temperature can be obtained by assuming polynomial approximation as

$$\log_{10}(\rho/\Omega\,\mathrm{cm}) = \sum_{i=0}^{m} a_i(T) \times \log_{10}([\mathrm{Al}]/\mathrm{cm}^{-3})^i. \quad (1)$$

Here, ρ is the resistivity, a_i is the fitting coefficient, T is the absolute temperature, and [Al] is the aluminum doping concentration. From this equation, fitting curves can be acquired and indicated in Fig. 2(a) with colored solid lines in the case of $m = 1$.

The coefficients a_0 and a_1 are determined by the least-squares method at individual temperatures and presented in Fig. 3. The absolute values of the coefficients a_0 and a_1 increase with the temperature, which reflects the increase of the resistivity in the lightly doped p-type SiC ($<2.0 \times 10^{16}$ cm^{-3}) at high temperatures because a_0 and a_1 represent the intercept and slope of fitting lines, respectively. As mentioned above, the increased resistivity in the lightly doped p-type SiC at high temperatures arises mainly from the decrease in mobility because almost all acceptors are ionized. Hence, both coefficients saturate above 600 K because hole mobility weakly depends on temperature at such a high temperature. The coefficient a_1 roughly saturates to minus unity, indicating that resistivity is proportional to the inverse of Al concentration, which is attributed to the complete ionization and the small temperature dependence of the hole mobility at high temperature. By utilizing the coefficients a_0 and a_1 obtained from the experimental results, the dependence of resistivity on doping concentration can be estimated at each measurement temperatures. However, besides the coefficients at the measurement temperatures, the coefficients at any temperatures should be known to acquire the dependence of resistivity on doping concentration at arbitrary temperatures.

Table I. Fitting coefficient b_{ij} for Eq. (2). The coefficient a_i in Eq. (1) can be traced by using a third-order polynomial approximation in Eq. (2). The applicable ranges of these coefficients for doping concentration and temperature are 1.5×10^{15}–$5.5 \times 10^{17}\,\mathrm{cm}^{-3}$ and 300–900 K, respectively.

b_{ij}	$j = 0$	1	2	3
$i = 0$	-3.81×10^{0}	7.79×10^{-2}	-9.24×10^{-5}	3.69×10^{-8}
1	3.27×10^{-1}	-5.04×10^{-3}	6.22×10^{-6}	-2.57×10^{-9}

Since the series of data points of the coefficient a_i is affluent, we assume that the coefficient at an arbitrary temperature between 293 and 900 K can be figured out by obtaining an analytical formula for the temperature-dependent coefficient a_i. In fact, the temperature dependence of the coefficient can be traced by using a third-order polynomial approximation as

$$a_i(T) = \sum_{j=0}^{n} b_{ij} \times T^j. \quad (2)$$

Here, b_{ij} is the fitting coefficient for a_i ($n = 3$). Thus, the temperature dependence of the coefficient a_i can be presumed by utilizing b_{ij} values, leading to the determination of resistivity at arbitrary temperatures and doping concentrations.

The b_{ij} values for the fitting coefficient a_i were determined by the least-squares method and are summarized in Table I. The fitting results are indicated in Fig. 3 by black (a_0) and red (a_1) solid lines, which agreed well with the coefficient a_i obtained by the process mentioned above. From Eqs. (1) and (2), and Table I, the temperature dependence of resistivity at the doping concentrations experimentally investigated can be calculated and several representative curves ([Al] = 2.0×10^{16} and $3.0 \times 10^{17}\,\mathrm{cm}^{-3}$) are plotted with colored dotted lines in Fig. 1. All of the fitting curves from 300 to 900 K are in relatively good agreement with the experimental resistiv-

Table II. Fitting coefficient b_{ij} for Eq. (2). For the accurate determination of resistivity, the presented values with the significant digit of eight should be input precisely because resistivity is very sensitive to the fitting coefficient a_i in Eq. (1). The applicable ranges of these coefficients for doping concentration and temperature are expanded to 5.8×10^{14}–$7.1 \times 10^{18}\,\mathrm{cm^{-3}}$ and 250–900 K, respectively.

b_{ij}	$j=0$	1	2	3	4	5	6
$i=0$	-3.8713528×10^{3}	4.2487692×10^{1}	$-1.7998246 \times 10^{-1}$	3.8533797×10^{-4}	$-4.4873183 \times 10^{-7}$	$2.7251689 \times 10^{-10}$	$-6.7889561 \times 10^{-14}$
1	7.0459471×10^{2}	-7.7583612×10^{0}	3.3129045×10^{-2}	$-7.1547922 \times 10^{-5}$	8.4102986×10^{-8}	$-5.1587332 \times 10^{-11}$	$1.2985038 \times 10^{-14}$
2	-4.2406555×10^{1}	4.6867048×10^{-1}	$-2.0156622 \times 10^{-3}$	4.3872158×10^{-6}	$-5.1997984 \times 10^{-9}$	$3.2169850 \times 10^{-12}$	$-8.1685031 \times 10^{-16}$
3	8.4579967×10^{-1}	$-9.3826374 \times 10^{-3}$	4.0608791×10^{-5}	$-8.9006925 \times 10^{-8}$	$1.0626928 \times 10^{-10}$	$-6.6243121 \times 10^{-14}$	$1.6947511 \times 10^{-17}$

ities in p-type SiC with the wide-range doping concentrations from 1.5×10^{15} to $5.5 \times 10^{17}\,\mathrm{cm^{-3}}$ (the error is less than 35%). This analytical formula can be incorporated in device or circuit simulations to practically reproduce temperature-dependent resistivity. It should be noted that the error becomes large when the doping concentration and temperature are out of the designated range, and the compensation ratio should be low enough for an accurate estimation. In particular, the resistivity of the Al^+-implantation region must be at least 10% higher than the value predicted from the analytical formula due to high compensation ratio and incomplete electrical activation of the implanted Al atoms.[20,31)]

In order to minimize the fitting errors of the resistivity further, the order of the polynomial approximation in Eq. (1) was increased to three ($m = 3$), the fitting results of which are demonstrated in Fig. 2(b). In this case, the applied ranges of the doping concentration and temperature for the fitting were expanded to 5.8×10^{14}–$7.1 \times 10^{18}\,\mathrm{cm^{-3}}$ and 250–900 K, respectively. Although the fitting error is improved, the temperature dependence of the coefficients (a_0–a_3) must be traced by using a sixth order polynomial approximation [$n = 6$ in Eq. (2)]. The b_{ij} values for the fitting coefficient a_i are summarized in Table II. Resistivity is so sensitive to the fitting coefficients a_i that the significant digit of the b_{ij} values should be large, at least eight. We confirmed that the fitting curves for the resistivity obtained from Eqs. (1) and (2), and Table II can well reproduce the experimental results in the designated ranges of the doping concentration and temperature (the error becomes less than 10%). Several representative curves ($[\mathrm{Al}] = 5.8 \times 10^{14}$, 2.0×10^{16}, 3.0×10^{17}, and $7.1 \times 10^{18}\,\mathrm{cm^{-3}}$) are plotted with the colored solid lines in Fig. 1.

Figure 4 shows the temperature dependence of resistivity normalized by the value at 293 K. The symbols denote the experimental data. For fabricating a resistor of high-temperature integrated circuits, temperature-independent resistivity is ideal. The suitable doping concentration can be suggested by utilizing the proposed analytical formula. The black solid line in Fig. 4 is normalized resistivity in p-type SiC with a doping concentration of $1.7 \times 10^{17}\,\mathrm{cm^{-3}}$ derived from the calculation with Eqs. (1) and (2), and Table II. The decrease in mobility at the elevated temperature is most effectively compensated by the increase in hole concentration, leading to the smallest dependence on temperature. The $\Delta\rho/\rho_{RT}$ ratio is within 35% in the entire temperature region from 300 to 900 K, where ρ_{RT} and $\Delta\rho$ denote resistivity at 293 K and the difference in resistivity from ρ_{RT}, respectively. Although resistivity in a highly doped n-type Si shows a small $\Delta\rho/\rho_{RT}$ ratio of less than 5%,[28)] temperature is limited to below

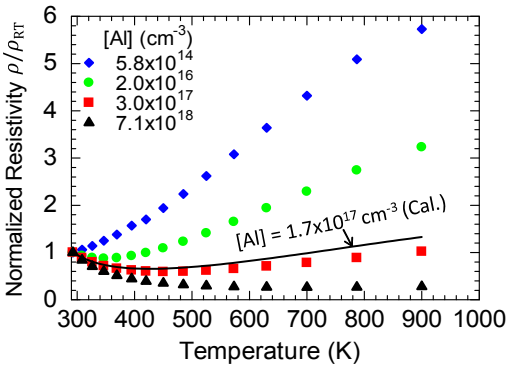

Fig. 4. (Color online) Temperature dependence of the resistivity of p-type SiC, which is normalized by the value at 293 K. The symbols are obtained from the experiment. The normalized resistivity of p-type SiC with a doping concentration of $1.7 \times 10^{17}\,\mathrm{cm^{-3}}$ is calculated from Eqs. (1) and (2), and Table II, as indicated by the black line.

500 K. Thus, the small $\Delta\rho/\rho_{RT}$ ratio of p-type SiC in the wide temperature range is unique to p-type SiC, which is attributed to the incomplete ionization of Al acceptors at moderate temperatures. The resistivity of p-type SiC above 500 K with a doping concentration of $6.8 \times 10^{18}\,\mathrm{cm^{-3}}$ is least dependent on temperature (not shown). Since resistivity with a small temperature dependence is required to design high-temperature integrated circuits, the knowledge obtained in this study is significantly important and practical.

The temperature dependence of resistivity in p-type SiC with the doping concentration of $5.8 \times 10^{14}\,\mathrm{cm^{-3}}$ above 300 K (blue diamonds in Fig. 4) reflects the temperature dependence of hole mobility because almost all acceptors are already ionized at 300 K. The dominant carrier scattering mechanism in the lightly doped p-type SiC below 400 K is acoustic phonon scattering, and optical phonon scattering appends at a higher temperature, resulting in the radical increase in normalized resistivity from 400 to 600 K.[20,21,26)] At temperatures above 600 K, the carrier scattering mechanism is predominated by optical phonon scattering and the temperature dependence of mobility decreases.

In summary, the temperature dependence of resistivity in p-type 4H-SiC with various doping concentrations (5.8×10^{14}–$7.1 \times 10^{18}\,\mathrm{cm^{-3}}$) was presented. The analytical formula of the polynomial approximation for resistivity was derived from the obtained data. The fitting formula enables accurate estimation of resistivity in p-type 4H-SiC with wide-range doping concentrations at an arbitrary temperature from 250 to 900 K. This work provides the convenient data and analytical formula for designing SiC devices operating in a wide temperature range.

1) M. Bhatnagar and B. J. Baliga, IEEE Trans. Electron Devices **40**, 645 (1993).
2) M. Ruff, H. Mitlehner, and R. Helbig, IEEE Trans. Electron Devices **41**, 1040 (1994).
3) A. Itoh, T. Kimoto, and H. Matsunami, IEEE Electron Device Lett. **17**, 139 (1996).
4) C. E. Weitzel, J. W. Palmour, C. H. Carter, K. Moore, K. J. Nordquist, S. Allen, C. Thero, and M. Bhatnagar, IEEE Trans. Electron Devices **43**, 1732 (1996).
5) J. A. Cooper, M. R. Melloch, R. Singh, A. Agarwal, and J. W. Palmour, IEEE Trans. Electron Devices **49**, 658 (2002).
6) H. Niwa, J. Suda, and T. Kimoto, Appl. Phys. Express **5**, 064001 (2012).
7) H. Miyake, T. Kimoto, and J. Suda, IEEE Electron Device Lett. **32**, 841 (2011).
8) G. Y. Chung, C. C. Tin, J. R. Williams, K. McDonald, R. K. Chanana, R. A. Weller, S. T. Pantelides, L. C. Feldman, O. W. Holland, M. K. Das, and J. W. Palmour, IEEE Electron Device Lett. **22**, 176 (2001).
9) J. Wang, T. Zhao, J. Li, A. Q. Huang, R. Callanan, F. Husna, and A. Agarwal, IEEE Trans. Electron Devices **55**, 1798 (2008).
10) A. Salemi, H. Elahipanah, K. Jacobs, C.-M. Zetterling, and M. Östling, IEEE Electron Device Lett. **39**, 63 (2018).
11) R. Hedayati, L. Lanni, S. Rodriguez, B. G. Malm, A. Rusu, and C.-M. Zetterling, IEEE Electron Device Lett. **35**, 693 (2014).
12) P. G. Neudeck, D. J. Spry, L.-Y. Chen, G. M. Beheim, R. S. Okojie, C. W. Chang, R. D. Meredith, T. L. Ferrier, L. J. Evans, M. J. Krasowski, and N. F. Prokop, IEEE Electron Device Lett. **29**, 456 (2008).
13) S. Kargarrazi, L. Lanni, S. Saggini, A. Rusu, and C.-M. Zetterling, IEEE Trans. Electron Devices **62**, 1953 (2015).
14) P. G. Neudeck, R. S. Okojie, and L.-Y. Chen, Proc. IEEE **90**, 1065 (2002).
15) W. Götz, A. Schöner, G. Pensl, W. Suttrop, W. J. Choyke, R. Stein, and S. Leibenzeder, J. Appl. Phys. **73**, 3332 (1993).
16) J. Pernot, S. Contreras, J. Camassel, J. L. Robert, W. Zawadzki, E. Neyret, and L. D. Cioccio, Appl. Phys. Lett. **77**, 4359 (2000).
17) H. Iwata and K. M. Itoh, J. Appl. Phys. **89**, 6228 (2001).
18) J. Pernot, W. Zawadzki, S. Contreras, J. L. Robert, E. Neyret, and L. D. Cioccio, J. Appl. Phys. **90**, 1869 (2001).
19) S. Kagamihara, H. Matsuura, T. Hatakeyama, T. Watanabe, M. Kushibe, T. Shinohe, and K. Arai, J. Appl. Phys. **96**, 5601 (2004).
20) A. Parisini and R. Nipoti, J. Appl. Phys. **114**, 243703 (2013).
21) A. Koizumi, J. Suda, and T. Kimoto, J. Appl. Phys. **106**, 013716 (2009).
22) H. Matsuura, K. Sugiyama, K. Nishikawa, T. Nagata, and N. Fukunaga, J. Appl. Phys. **94**, 2234 (2003).
23) G. Pensl, F. Schmid, F. Ciobanu, M. Laube, S. A. Reshanov, N. Schulze, K. Semmeiroth, H. Nagasawa, A. Schöner, and G. Wagner, Mater. Sci. Forum **433–436**, 365 (2003).
24) S. Asada, T. Okuda, T. Kimoto, and J. Suda, Appl. Phys. Express **9**, 041301 (2016).
25) S. Asada, T. Kimoto, and I. G. Ivanov, Appl. Phys. Lett. **111**, 072101 (2017).
26) H. Tanaka, S. Asada, T. Kimoto, and J. Suda, to be published in J. Appl. Phys.
27) S. N. Mohammad, A. V. Bemis, R. L. Carter, and R. B. Renbeck, Solid-State Electron. **36**, 1677 (1993).
28) S. S. Li and W. R. Thurber, Solid-State Electron. **20**, 609 (1977).
29) R. F. Schmucker and L. M. Scarfone, Solid-State Electron. **26**, 923 (1983).
30) W. M. Bullis, F. H. Brewer, C. D. Kolstad, and L. J. Swartzendruber, Solid-State Electron. **11**, 639 (1968).
31) T. Kimoto, O. Takemura, and H. Matsunami, J. Electron. Mater. **27**, 358 (1998).